

Advanced Control for Active Magnetic Bearing

(Robust Control for flexible Rotor Magnetic Bearing Considering Spillover and Gyroscopic Effects)

Tomoaki Takami

takami@mi-3.mech.kobe-u.ac.jp

Michihiro Kawanishi

kawa@mech.kobe-u.ac.jp

Hiroshi Kanki

kanki@mech.kobe-u.ac.jp

Department of Mechanical Engineering, Kobe University
Kobe city, Hyogo Prefecture, Japan

Abstract : In this paper, methods of designing a robust controller are proposed to solve spillover and gyro problems. A control system is designed based on a H_∞ Loop Shaping Design Procedure. By shaping open loop properly, the designer can stabilize high order modes while giving low order modes to enough damping. A Hadamard weight is added to attenuate coupling caused by gyroscopic effects. The effectiveness of the proposed method is confirmed by experiments.

1 INTRODUCTION

Most rotating machinery with active magnetic bearings(AMB) are designed as rigid rotors. However, they should be treated as flexible during high speed operation. In designing controller for magnetic bearing, it is needed to give enough damping to eigen-frequencies in the range of operation speed and to stabilize high order modes. The flexible rotor has two rigid modes and many flexible modes. In designing controllers, however, a rotor model representing dominant low order modes has been used because of the difficulty of identifying high order modes and controller complexity limitation. This methodology introduce the possibility that the controller excites higher modes and unstable vibration, so called spillover. In addition, the inclination of the rotor makes gyroscopic effects in case of the flexible rotor.

In this paper, a design method of a robust control system is proposed based on the H_∞ loop shaping method^{[1][2]}. The loop shaping method in classical control was difficult for multivariable systems. Then McFarlane and Glover proposed to combine the classical one with solutions of H_∞ control problem. In this method, only the gain curve of the plant is shaped around low and high frequencies and a stabilizing con-

troller is designed by solving the H_∞ control problems. It can be possible to keep high order modes stable and give low order modes enough damping by shaping properly.

Hadamard weight is added to attenuate coupling by gyroscopic effects. This is added by Hadamard product which is possible to multiply element by element. Therefore it can suppress the effect of off-diagonal elements of the closed-loop without weighting the on-diagonal elements. It is confirmed by experiments that the proposed method is effective for spillover. Simulation evaluates the Hadamard weight is effective for decoupling.

2 EXPERIMENTAL SETUP

In this section, flexible rotor magnetic bearing system is explained taking experimental setup as example.

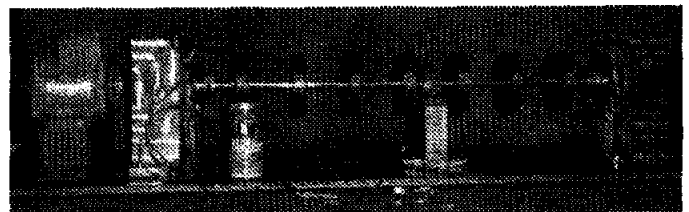


Figure 1: Experimental setup

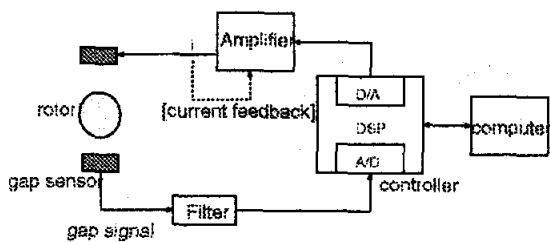


Figure 2: AMB system

Fig.1 shows the picture of the experimental setup. The rotor has 9 disks. It is supported by the AMB at each edge. The gap is 0.4mm when the rotor levitates at the center. The bias current is 1.65A. Fig.2 shows sketch of the AMB system. In this AMB, push-pull coil configuration is used.

3 SPILLOVER AND GYROSCOPIC EFFECTS

Spillover phenomena is demonstrated in experimental apparatus. Testing attempts are to levitate the rotor with 9 disks with conventional PID controllers (P:12000 I:2000 D:21). Unstable vibration occurred as shown in Fig.3. FFT analysis shows that the resonant frequencies are 110, 255 and 330Hz, which is shown in Fig.4.

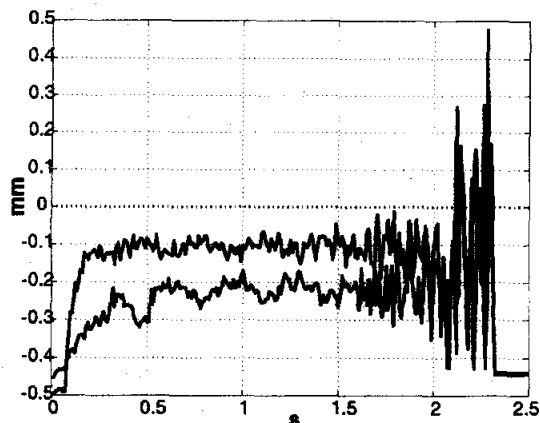


Figure 3: Levitation experiment

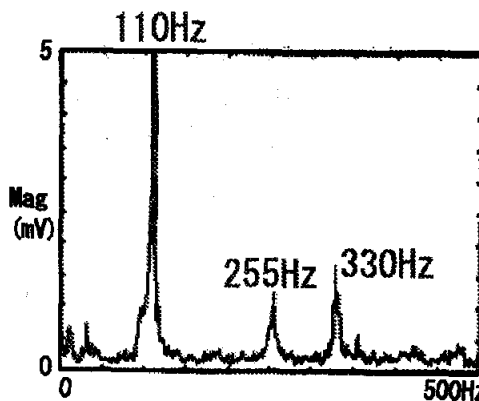


Figure 4: Vibration spectrum

The PID controller has a frequency response curve as indicated by solid lines in Fig.5. However characteristics of the coil in the electro-magnetic and DSP decrease the gain and give the phase-lag at high frequencies as shown by dotted lines in the same figure. The problem is that the phase becomes negative above about 55Hz although the gain is still high. In other words, above 55Hz the controller gives the plant negative damping. In Fig.6, the plot for theoretical closed loop poles shows that two poles are in the right half plane and it is satisfactory to consider one of them (111.8Hz) to be the cause of vibration. Even if phase-lead is added, gain in higher frequency become high, which causes noise problem and excitation of high order modes. In this way, it is difficult to stabilize all modes and it requires repeated parameter selection.

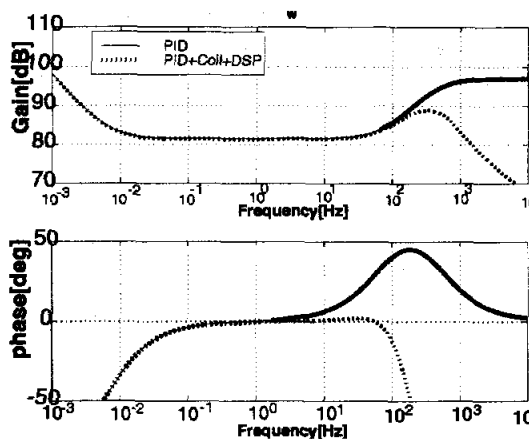


Figure 5: Bode diagrams of PID controller

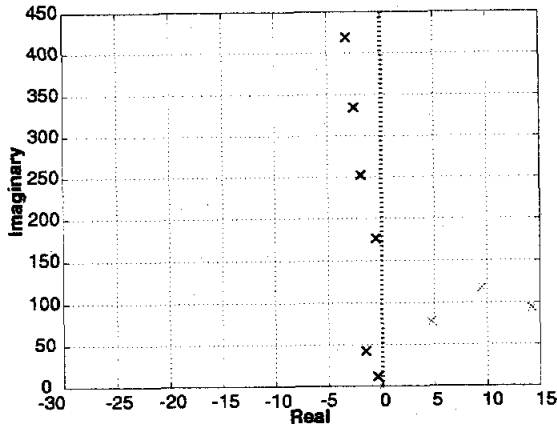


Figure 6: Closed loop poles in spillover phenomenon

In flexible rotor, gyroscopic effects cause coupling and deteriorate control performance. Disturbance test was simulated to examine this effects. The disturbance was added to the vertical way at one side of the rotor as impulse of current 5[A]. The rotating speed of the rotor is 10000[rpm]. Fig.7 shows that disturbance have influence on horizontal way as well as vertical way due to gyroscopic effects.

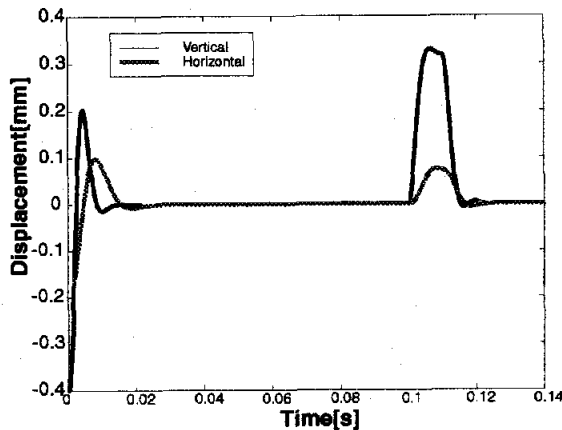


Figure 7: Simulation result

4 MATHEMATICAL MODEL

In this section, a mathematical model of the magnetic bearing system is introduced.

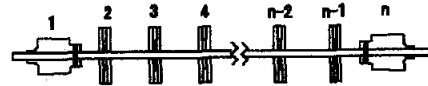


Figure 8: The rotor with n disks

For a rotor with n disks as seen in Fig.8, dynamic equation is constructed by replacing each disk with centralized mass. Nonlinearity of the magnetic force is linearized by first-order approximation around balanced point. If internal damping is not taken into consideration, the dynamic equation is

$$M\ddot{q} + J_p\Omega\dot{q} + Kq = \Gamma K_i \tilde{i} + \Gamma K_m \Gamma^T q. \quad (1)$$

The vector q consists of displacement and slope at each disk. M , J_p , K and Γ are the mass, the gyro, the stiffness and the position matrix, respectively. Ω , K_i , K_m and \tilde{i} are the rotating speed([rad/sec]), the force coefficient of the electromagnet([N/A]), the negative stiffness([N/m]) and the control current([A]), respectively.

Applying modal transformation with $q = \Phi\xi$, Eq.(1) is transformed to

$$\ddot{\xi} + J'_p\Omega\dot{\xi} + \omega^2\xi = (\Phi^T\Gamma K_i)\tilde{i}, \quad (2)$$

where ω is modal eigen-frequency and $J'_p = \Phi^T J_p \Phi$.

To consider the internal damping, introducing rotational coordinate system with $\xi = \eta e^{j\Omega t}$ and adding internal damping term $2\omega\zeta\dot{\eta}$, where ζ is modal damping, the Eq.(2) is transformed into

$$\ddot{\eta} + (2j\Omega + 2\omega\zeta + J'_p\Omega)\dot{\eta} + (\omega^2 - \Omega^2 + jJ'_p\Omega^2)\eta = (\Phi^T\Gamma K_i)\tilde{i}e^{-j\Omega t}. \quad (3)$$

Free free test was carried out to check the error of model and experimental setup. It is shown in Table 1 that the error is under 4% and this model is adequate.

Table 1: Comparison of natural frequencies

	experimental[Hz]	theoretical[Hz]	error[%]
1&2	0	0	0
3	20.0	20.4	2.0
4	55.0	56.8	3.3
5	107.7	110.0	2.1
6	172.5	176.5	2.3
7	256.4	252.5	1.5
8	343.7	334.4	2.7
9	427.4	419.6	1.8

5 ROBUST CONTROL AND DESIGN METHOD

In this section, proposed robust control design method is explained.

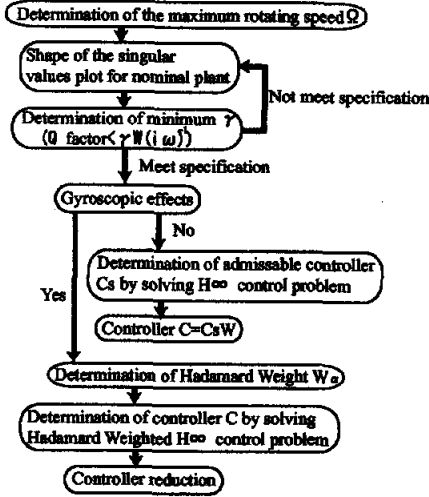


Figure 9: Flowcharts

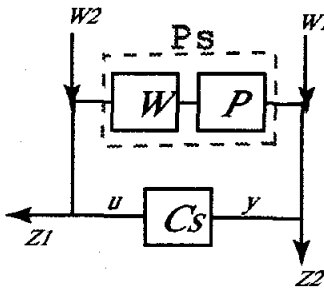


Figure 10: Feedback control system

Fig.9 shows flowcharts of proposed method. The detailed procedure is as follows.

STEP1)

The upper limitation of rotating speed is determined to consider deterioration of internal damping.

STEP2)

As seen in Fig.10, plant $P(s)$ is shaped by $W(s)$ which is defined as

$$W(s) = \left(W_P + \frac{W_I}{s} \right) \frac{\left(\frac{1}{2\pi f_{n1}} s + 1 \right) \cdots \left(\frac{1}{2\pi f_{nm}} s + 1 \right)}{\left(\frac{1}{2\pi f_{d1}} s + 1 \right) \cdots \left(\frac{1}{2\pi f_{dl}} s + 1 \right)} I_4. \quad (4)$$

Parameters of the $W(s)$ are chosen as follows:

W_P is determined so that the eigen-frequency of the 1st mode

$$\omega_1 \approx \frac{1}{2\pi} \sqrt{\frac{2(K_i W_P - K_m)}{M}} [Hz] \quad (5)$$

becomes about 90% of the eigen-frequency which obtained experimentally.

W_I is determined so that the designed magnetic bearings have a certain amount of static stiffness.

$f_{n1}, \dots, f_{nm}, f_{d1}, \dots, f_{dl}$ ($m \leq l$) are determined so that the gain at high frequency becomes low and the shaped plant have a roll-off of apploximately 20dB/dec at the desired bandwidth.

STEP3)

The minimum value of γ is calculated in

$$\gamma_{min} = \sqrt{1 + \lambda_{max}(ZX)}, \quad (6)$$

where Z, X are the solution of two Riccati equations expressed on

$$(A_s - B_s s^{-1} D_s^T C_s)^T X + X (A_s - B_s s^{-1} D_s^T C_s) - X B_s s^{-1} B_s^T X + C_s^T R^{-1} C_s = 0 \quad (7)$$

and

$$(A_s - B_s D_s^T R^{-1} C_s) Z + Z (A_s - B_s D_s^T R^{-1} C_s)^T - Z C_s^T R^{-1} C_s Z + B_s s^{-1} B_s^T = 0, \quad (8)$$

where A_s, B_s, C_s, D_s are minimum realization of the shaped plant $P_s(s)$, $S = I + D_s^T D_s, R = I + D_s D_s^T$.

γ_{min} is related with Q factor as $Q < \gamma_{min} |W(i\omega)^{-1}|$. If it does not meet specification, the plant should be shaped again.

STEP4)

When gyroscopic effects are not considered, the stabilizing controller $C_s(s)$ is obtained by solving H_∞ control problem^{[1][2]}. Final controller is designed as $C(s) = C_s(s)W(s)$.

When gyroscopic effects cause coupling to the plant, a Hadamard weight^[3] should be added to the plant as $W_\alpha \circ F_l(G(s), C(s))$, where \circ is symbol of Hadamard product, F_l is Linear Fractional Transformation and $G(s)$ is generalized plant. The Hadamard weight makes it possible to suppress the effect of off-diagonal elements of the closed-loop without weighting the on-diagonal elements. For example, in our experimental setup of 4 input 4 output, the Hadamard weight is determined as

$$W_\alpha = \begin{bmatrix} 1 & 1 & 1 & 1 & 1 & 1 & 1 & 1 \\ 1 & 1 & 1 & 1 & 1 & 1 & 1 & 1 \\ 1 & 1 & 1 & 1 & 1 & 1 & 1 & 1 \\ 1 & 1 & 1 & 1 & 1 & 1 & \alpha & \alpha \\ 1 & 1 & 1 & 1 & 1 & 1 & \alpha & \alpha \\ 1 & 1 & 1 & 1 & \alpha & \alpha & 1 & 1 \\ 1 & 1 & 1 & 1 & \alpha & \alpha & 1 & 1 \end{bmatrix} \quad (9)$$

to suppress the effect from w_2 to z_2 in Fig.10, where α is tuned to change level of decoupling. Stabilizing controller $C(s)$ are obtained by solving Hadamard weighted

H_∞ control problems^[4]. In this method, there is problem which the degree of controller becomes large. In our experimental setup, it is 1384. By Hankel norm approximation, it was reduced into 19 degree to apply to real system, but the characteristic had been changed as seen from singular values plot of reduced controller in Fig.11. To avoid this, frequency-dependent weights are added so that reduction error concentrate on low frequency domain which does not require exact reduction. Fig.12 shows singular values plot for reduced controller with weight. It is clear that characteristics around 10Hz has been improved.

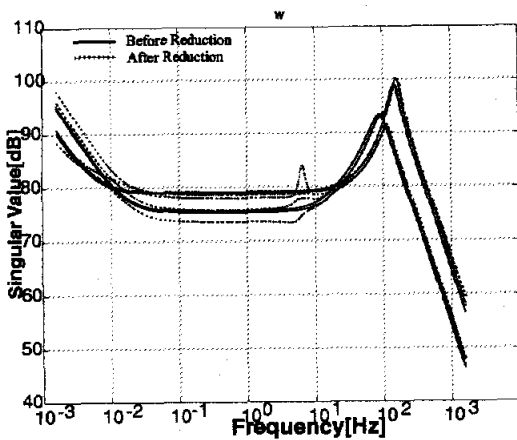


Figure 11: Reduction of controller

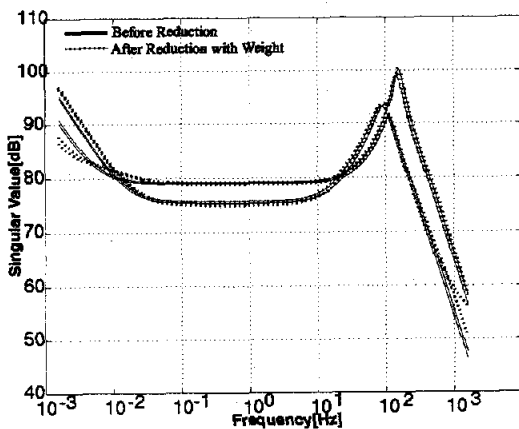


Figure 12: Reduction with weights

6 DISCUSSION

Based on proposed method, controller is designed. A compensator for shaping is chosen as

$$W(s) = \left(6.5 \times 10^4 + \frac{60000}{s} \right) \frac{\left(\frac{1}{2\pi 150} s + 1 \right) \left(\frac{1}{2\pi 150} s + 1 \right)}{\left(\frac{1}{2\pi 30} s + 1 \right) \left(\frac{1}{2\pi 200} s + 1 \right)} I_2 \quad (10)$$

Fig.13 shows bode diagrams of designed controller with PID controller.

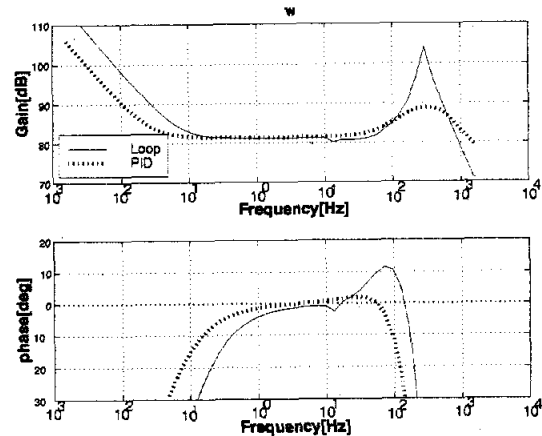


Figure 13: Bode diagrams

γ_{min} is 8.37 and all eigen-frequencies has been stabilized as seen in Fig.14

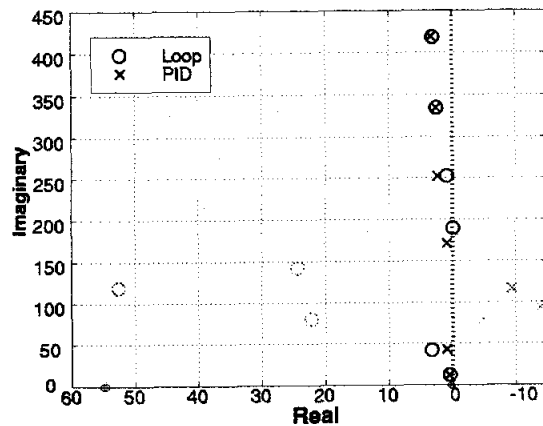


Figure 14: Closed loop poles

Next the Hadamard weighted controller is designed to attenuate coupling. The weighting factor α is 10. Bode diagrams of the controller was shown in Fig.12. Same disturbance test as Fig.?? was simulated to examine the effect of Hadamard weight. It is clear from

Fig.15 that coupling is attenuated by Hadamard weight. The max stability margin ϵ is influenced by this weight. It is expressed as

$$\epsilon = \left\| \left[\begin{array}{c} C_s(s) \\ I \end{array} \right] (I - P_s(s)C_s(s))^{-1} \left[\begin{array}{cc} I & P_s(s) \end{array} \right] \right\|_{\infty}^{-1} \quad (11)$$

For $\alpha = 0, \alpha = 10$, stability margin is $\epsilon_{\alpha=0} = 0.237, \epsilon_{\alpha=10} = 0.221$. The Hadamard weight does not make stability margin worse so much.

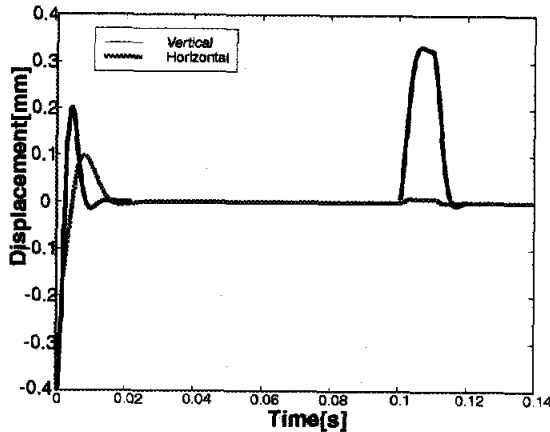


Figure 15: Simulation (with Hadamard weight)

7 EXPERIMENTAL RESULTS

Levitation and rotating tests were carried out to confirm effects of proposed method. Experimental setup was shown in Fig.1. Fig.16 shows displacement of the rotor after levitation. By using robust controller, spillover did not occur.

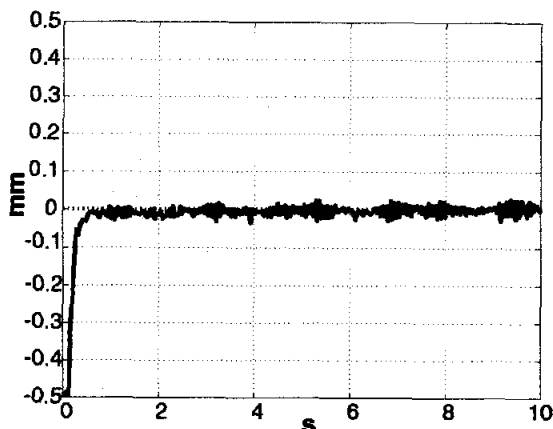


Figure 16: Levitation experiments

After levitation, the rotor was rotated by the mo-

tor. It can be seen from Fig.17 that the rotor rotates across the 1st and the 2nd mode's resonant frequencies (650rpm, 1800rpm).

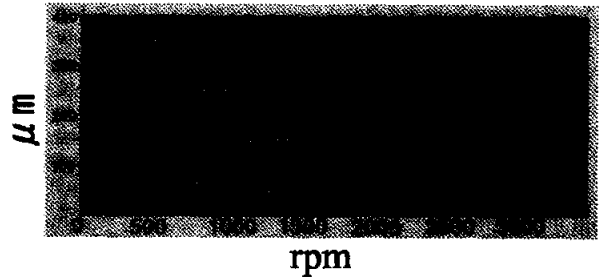


Figure 17: Rotating experiments

8 CONCLUSION

In this paper, a control system design method for flexible rotor magnetic bearing was proposed to prevent spillover and attenuate coupling by gyroscopic effects. The design method is based on the H_{∞} loop shaping method. Using Hadamard weight, decoupling control system was designed. In experiment, the rotor rotates across the 1st and the 2nd mode's resonant frequencies. In simulation, it was confirmed that Hadamard weight is effective for coupling by gyroscopic effects.

References

- [1] D.McFarlane and K.Glover. A Loop Shaping Design Procedure Using H_{∞} Synthesis. *IEEE Transactions on Automatic Control*, Vol. 37, No. 6, pp. 759-769, July 1992.
- [2] K.Glover and D.McFarlane. Robust Stabilization of Normalized Coprime Factor Plant Descriptions with H_{∞} -Bounded Uncertainty. *IEEE Transactions on Automatic Control*, Vol. 34, No. 8, pp. 821-830, August 1989.
- [3] F.Van Diggelen and K. Glover. A Hadamard Weighted Loop Shaping Design Procedure for Robust Decoupling. *Automatica*, Vol. 30, No. 5, pp. 831-845, 1994.
- [4] F.Van Diggelen and K. Glover. State-space solutions to Hadamard weighted H_{∞} and H_2 control problems. *Int.J.Control*, Vol. 59, No. 2, pp. 357-394, 1994.